

Numerical Analyses of Weakly Nonlinear Velocity-Density Coupling

NAOKI SETO

Department of Earth and Space Science, Osaka University, Toyonaka 560-0043, Japan

NAOSHI SUGIYAMA

Division of Theoretical Astrophysics, National Astronomical Observatory, 181-8588, Japan

ABSTRACT

We study evolution of various statistical quantities of smoothed cosmic density and velocity fields using N-body simulations. The parameter $C \equiv \langle \mathbf{V}^2 \delta \rangle / (\langle \mathbf{V}^2 \rangle \langle \delta^2 \rangle)$ characterizes nonlinear coupling of these two fields and determines behavior of bulk velocity dispersion as a function of local density contrast. It is found that this parameter depends strongly on the smoothing scale even in quasi-linear regimes where the skewness parameter $S_3 \equiv \langle \delta^3 \rangle / \langle \delta^2 \rangle^2$ is nearly constant and close to the predicted value by the second-order perturbation theory. We also analyze weakly nonlinear effects caused by an adaptive smoothing known as the gather approach.

1. INTRODUCTION

It is now commonly accepted that the large-scale structure in the universe is gravitationally evolved from small initial inhomogeneities. In addition to redshift surveys of galaxies and temperature anisotropies of the cosmic microwave background radiation, observational analysis of the cosmic velocity field would bring us fruitful information of our universe, such as, the density parameter Ω_0 or the matter power spectrum (Dekel 1994, Strauss & Willick 1995). In order to analyze the velocity field, however, we need to clarify a basic problem, whether the velocity field of galaxies is statistically different from that of dark-matter particles. The observed line-of-sight peculiar velocity field is not usually traced by the underlying density field but by galaxies, since the measurements of the distances are crucial element to determine the peculiar velocity field and are usually carried by using galaxies. This important problem in observational cosmology is broadly called the velocity bias. The velocity bias is often studied using semi-analytic models of galaxy formation (Cen & Ostriker 1992, Kauffmann et al. 1999, Narayanan et al. 2000). But it is not easy to make definite predictions with this approach, because our understanding of astrophysical process related to galaxy formation reaches far from a quantitative level.

The number density of galaxies is expected to be closely related to the density contrast of dark matter. Therefore we can obtain some insights about the velocity bias by analyzing relation between the velocity and density fields only of dark matter particles. This analysis is relatively simple, as

only gravitation is the relevant physical process for their evolution. When the initial fluctuations are isotropic random Gaussian distributed, these two fields at a same point are statistically independent in the framework of the linear perturbation theory. One of the author (Seto 2000a) studied weakly nonlinear evolution of the bulk (smoothed) velocity dispersion $\Sigma_V^2(\delta)$ as a function of local smoothed density contrast δ . He used the Eulerian second-order perturbation theory and the Edgeworth expansion method, and found that the constrained velocity dispersion $\Sigma_V^2(\delta)$ is written in the form $\Sigma_V^2(\delta) \propto (1 + C\delta + O(\delta^2))$ with a parameter $C \simeq 0.2 \sim 0.3$ for typical CDM models (see also Chodorowski & Łokas 1997 for the velocity divergence field).

However, numerical results given in Kepner et al. (1997) show that magnitude of bulk velocity is almost independent on the local density contrast δ at nonlinear regimes (see their figs 2.a and 3.a). This behavior shows a remarkable difference from the above second-order prediction. Therefore we expect that the quantities C and $\Sigma_V^2(\delta)$ show interesting behaviors by changing a spatial scale from linear to nonlinear, and would be useful measures to check performance of the perturbative analysis for weakly nonlinear evolution of the large-scale structure. In this article we study these quantities using N-body simulations and compare numerical results with analytical second-order predictions.

This article is organized as follows. We begin by summarizing the second-order analysis of Seto (2000a) in §2.1. Smoothing operation is crucial for our numerical analysis and its proper treatment is very important to make a quantitative analysis. There are some variations for smoothing methods. A mass-weighted smoothing scheme is convenient for analyzing N-body data and an adaptive smoothing scheme might be efficient to resolve cosmic fields, especially in sparse underdense regions. We perturbatively study these methods in §2.2 and §2.3. In §3 we derive an expression to estimate the sampling fluctuation expected in our numerical analysis. Numerical results are given in §4. Finally §5 is devoted to a summary.

2. SECOND-ORDER PERTURBATION THEORY

2.1. Smoothed Velocity Dispersion as a Function of Local Density

In this subsection we summarize the perturbative analysis of density and velocity fields and their correlations given in Seto (2000a). We denote the volume-weighted smoothing operator $[\cdot]_R$ with radius R for a field $f(\mathbf{x})$ as follows:

$$[f(\mathbf{x})]_R \equiv \int d^3x' f(\mathbf{x}) W(\mathbf{x}' - \mathbf{x}; R), \quad (1)$$

where $W(\mathbf{x}, R)$ is a smoothing filter function. For simplicity we also use a notation $f_R(\mathbf{x}) \equiv [f(\mathbf{x})]_R$. In this article we only employ the Gaussian filter defined as

$$W(\mathbf{x}; R) = \frac{1}{(2\pi R^2)^{3/2}} \exp\left(-\frac{|\mathbf{x}|^2}{2R^2}\right), \quad (2)$$

and discuss velocity and density fields smoothed by this filter.

The smoothed (bulk) velocity dispersion $\Sigma_V^2(\delta)$ for points \mathbf{x} with a given smoothed overdensity $\delta_R(\mathbf{x}) = \delta$ is formally expressed as

$$\Sigma_V^2(\delta) = \frac{\langle \mathbf{V}_R(\mathbf{x})^2 \delta_D[\delta_R(\mathbf{x}) - \delta] \rangle}{\langle \delta_D[\delta_R(\mathbf{x}) - \delta] \rangle}, \quad (3)$$

where $\delta_D(\cdot)$ is the Dirac's delta function and the bracket $\langle \cdot \rangle$ represents an ensemble average. Let us evaluate this expression using the second-order Eulerian perturbation theory (Peebles 1980) and the Edgeworth expansion method (Matsubara 1994, Juszkiewicz et al. 1995, Bernardeau & Kofman 1995). We first expand the density and velocity fields as

$$\delta(\mathbf{x}) = \delta_1(\mathbf{x}) + \delta_2(\mathbf{x}) + \delta_3(\mathbf{x}) + \dots, \quad (4)$$

$$\mathbf{V}(\mathbf{x}) = \mathbf{V}_1(\mathbf{x}) + \mathbf{V}_2(\mathbf{x}) + \mathbf{V}_3(\mathbf{x}) + \dots, \quad (5)$$

where $\delta_1(\mathbf{x})$ and $\mathbf{V}_1(\mathbf{x})$ are the linear modes, $\delta_2(\mathbf{x})$ and $\mathbf{V}_2(\mathbf{x})$ are the second-order modes, and so on. We can regard the order parameter of these expansions as the rms density fluctuation $\sigma \equiv \langle \delta_R^2 \rangle^{1/2}$. We assume that the primordial fluctuation is isotropic random-Gaussian distributed and the linear modes $\delta_1(\mathbf{x})$ and $\mathbf{V}_1(\mathbf{x})$ obey this simple statistic. Then their probability distribution function $P(\delta_1, \mathbf{V}_1)$ is determined by their covariance matrix (*e.g.* Bardeen et al. 1986). Although the linear velocity field \mathbf{V}_1 is given in terms of the linear density field δ_1 as $\mathbf{V}_1 \propto \nabla \Delta^{-1} \delta_1$, this matrix is orthogonal due to the statistical isotropy of fluctuations. Thus these four variables (density and three components of velocity fields) are statistically independent, as long as we discuss the density and velocity fields at a same point. Therefore at the linear order, velocity dispersion does not depend on the density contrast δ and is given as

$$\Sigma_V^2(\delta) = \langle \mathbf{V}_{1R} \cdot \mathbf{V}_{1R} \rangle + O(\sigma^4). \quad (6)$$

Next we evaluate the higher order correction using the multivariable Edgeworth expansion for the one point probability distribution function $P(\delta, \mathbf{V})$ around its linear (gaussian) distribution. After some tedious algebra, we obtain the following expression up to the first non-Gaussian correction

$$\Sigma_V^2(\delta) = \langle \mathbf{V}_R^2 \rangle (1 + C\delta + O(\sigma^2)), \quad (7)$$

where the coefficient C is defined by

$$C \equiv \frac{\langle \mathbf{V}_R^2 \delta_R \rangle}{\langle \mathbf{V}_R^2 \rangle \langle \delta_R^2 \rangle}. \quad (8)$$

This coefficient C characterizes nonlinear couplings of the velocity and the density fields. Equation (7) shows that the first nonlinear correction for the velocity dispersion for points with a given density contrast δ is simply proportional to $C\delta$.

The leading order contributions for two factors $\langle \mathbf{V}_R \cdot \mathbf{V}_R \rangle$ and $\langle \delta_R^2 \rangle$ in the denominator of C are given in terms of the matter power spectrum $P(k)$ as follows

$$\langle \delta_R^2 \rangle = \int \frac{k^2 dk}{2\pi^2} P(k) W(kR)^2 + O(\sigma^4), \quad (9)$$

$$\sigma_V^2 \equiv \langle \mathbf{V}_R \cdot \mathbf{V}_R \rangle = H^2 f^2 \int \frac{dk}{2\pi^2} P(k) W(kR)^2 + O(\sigma^4), \quad (10)$$

where H is the Hubble parameter and f is a function of cosmological parameters Ω_0 and λ_0 , and well fitted by

$$f \simeq \Omega_0^{0.6} + \frac{\lambda_0}{70} \left(1 - \frac{\Omega_0}{2} \right), \quad (11)$$

in the ranges $0.03 \leq \Omega_0 \leq 2$ and $-5 \leq \lambda_0 \leq 5$ (Lahav et al. 1991). The function $W(kR)$ is a Fourier transformed filter with smoothing radius R . For the Gaussian filter (eq.[2]) we have $W(kR) = \exp(-k^2 R^2/2)$.

The ensemble average of an odd function of Gaussian variables (with vanishing means) leads to zero. We employ the second-order perturbation theory to evaluate the first nonvanishing contribution of the numerator $\langle \mathbf{V}_R \cdot \mathbf{V}_R \delta_R \rangle$. The leading order contribution for the numerator of C is written as

$$\langle \mathbf{V}_R \cdot \mathbf{V}_R \delta_R \rangle = \langle \mathbf{V}_{1R} \cdot \mathbf{V}_{1R} \delta_{2R} \rangle + 2 \langle \mathbf{V}_{1R} \cdot \mathbf{V}_{2R} \delta_{1R} \rangle + O(\sigma^6). \quad (12)$$

Using formulas for the second-order modes $\delta_2(\mathbf{x})$ and $\mathbf{V}_2(\mathbf{x})$ (e.g. Fry 1984, Goroff et al. 1986), the above expression is written with the matter power spectrum $P(k)$ as follows:

$$\begin{aligned} \langle \mathbf{V}_R \cdot \mathbf{V}_R \delta_R \rangle &= 2H^2 f^2 \int_{-1}^1 du \int \frac{k^2 l^2 dk dl}{8\pi^4} P(k) P(l) \exp[-(k^2 + l^2 + klu)R^2] \\ &\quad \times \left[-\frac{u}{kl} \left\{ \frac{5}{7} + \frac{u}{2} \left(\frac{k}{l} + \frac{l}{k} \right) + \frac{2}{7} u^2 \right\} \right. \\ &\quad \left. + 2 \frac{k + lu}{k(k^2 + l^2 + 2klu)} \left\{ \frac{3}{7} + \frac{u}{2} \left(\frac{k}{l} + \frac{l}{k} \right) + \frac{4}{7} u^2 \right\} \right] + O(\sigma^6). \end{aligned} \quad (13)$$

Here we have neglected extremely weak dependence on the cosmological parameters Ω_0 and λ_0 that appears in the kernels of the second-order modes. We should notice that the parameter $C = O(1)$ does not depend on normalization of the power spectrum at its first nonvanishing contribution (see eqs.[9][10] and [13]). The factors $(Hf)^2$ cancel out between the velocity dispersion σ_V^2 and the velocity-density moment $\langle \mathbf{V}_R \cdot \mathbf{V}_R \delta_R \rangle$. The parameter C is affected by the cosmological parameters mainly through its dependence on the power spectrum (e.g. the shape parameter $\Gamma \simeq \Omega h$ for CDM transfer function).

The parameter C characterizes the nonlinear mode couplings of velocity and density fields. It is interesting to compare this with a same kind of nonlinear quantity that is determined only by the density field δ . The skewness parameter $S_3 = O(1)$ is defined by the second- and third-order moments of density contrast δ and written as (Peebles 1980, Fry 1984, Bouchet et al. 1992, Juszkiewicz, Bouchet & Colombi 1993, Bouchet et al. 1993, Bernardeau 1994, Baugh, Gaztañaga & Efstathou 1995, Kim & Strauss 1998)

$$S_3 \equiv \frac{\langle \delta_R^3 \rangle}{\langle \delta_R^2 \rangle^2}. \quad (14)$$

Here the variance $\langle \delta_R^2 \rangle$ is given in equation (9). For unsmoothed density field we have $S_3 = 34/7$ (Peebles 1980). After some algebra we can express the third-order moment $\langle \delta_R^3 \rangle$ (Gauss filter) in terms of matter power spectrum $P(k)$ as follows

$$\begin{aligned} \langle \delta_R^3 \rangle = 6 \int_{-1}^1 du \int \frac{k^2 l^2 dk dl}{8\pi^4} P(k) P(l) \exp[-(k^2 + l^2 + klu)R^2] \\ \times \left[\left\{ \frac{5}{7} + \frac{u}{2} \left(\frac{k}{l} + \frac{l}{k} \right) + \frac{2}{7} u^2 \right\} \right] + O(\sigma^6). \end{aligned}$$

The skewness parameter and its generalizations are very important to study various aspects of weakly nonlinear density field. With these parameters we can discuss evolution of one-point PDF (Juszkiewicz et al. 1995, Bernardeau & Kofman 1995) or statistics of isodensity contour, such as, genus or area statistics (Matsubara 1994). It is known that the skewness parameter S_3 obtained from numerical simulations shows a good agreement with second-order prediction up to regime $\sigma^2 \simeq 1$ (*e.g.* Hivon et al. 1995, Juszkiewicz et al. 1995, Baugh, Gaztañaga & Efstathou 1995, Lokas et al. 1995). This fact is often used as a basis for reliability of second-order analysis.

The skewness parameter has been also studied observationally using various galaxy surveys (see Table 1 of Hui & Gaztañaga 1998). As we cannot observe the dark matter distribution $\delta(\mathbf{x})$ directly, the relation between the number density fluctuation of galaxies $\delta_g(\mathbf{x})$ and that of underlying matter $\delta(\mathbf{x})$ is crucially important to interpret the observed data. Their relation is called biasing and detailed theory of galaxy formation is required to understand it quantitatively. If the biasing relation is phenomenologically expressed as

$$\delta_g(\mathbf{x}) = b_1 \delta(\mathbf{x}) + \frac{b_2}{2} (\delta(\mathbf{x})^2 - \langle \delta(\mathbf{x})^2 \rangle) + \dots, \quad (15)$$

with numerical coefficients b_i , the first-order contribution of skewness parameter for the galaxy distribution $\delta_g(\mathbf{x})$ becomes (Fry & Gaztañaga 1994)

$$\frac{\langle \delta_g^3 \rangle}{\langle \delta_g^2 \rangle^2} = \frac{1}{b_1} \left(S_3 + \frac{3b_2}{b_1} \right). \quad (16)$$

When we discuss velocity dispersion as a function of galaxy overdensity δ_g , the coefficient C becomes (Seto 2000a)

$$\frac{\langle \delta_g \mathbf{V}^2 \rangle}{\langle \delta_g^2 \rangle \langle \mathbf{V}^2 \rangle} = \frac{C}{b_1}. \quad (17)$$

Note that the above expression does not depend on the coefficient b_2 .

In the following subsections we study various second-order effects of the moments S_3 and C caused by smoothing operation. We denote results derived in this subsection by S_{3V} and C_V with subscript V to specify the smoothing method which we employ, *i.e.*, the simple volume-weighted smoothing method.

In Tables 1, 2 we present numerical values of C_V and S_{3V} for power-law models smoothed by Gaussian filter. The parameter S_{3V} are given explicitly in terms of the Hypergeometric functions (Matsubara 1994, Lokas et al. 1995). For the top-hat filter we obtain simple expression as $S_{3V} = 34/7 - (n + 3)$ (e.g. Bernardeau 1994).

2.2. Second-Order Correction for the Mass-Weighted Smoothed Velocity Field

In the previous subsection we have discussed the smoothed (bulk) velocity dispersion as a function of the smoothed density contrast δ . Following standard procedure of the Eulerian perturbation theory, we have adopted the volume-weighted smoothing method (eq.[1]). However it is not a simple task to obtain the volume-weighted velocity field from N-body simulations due to their Lagrangian nature (Bernardeau & van de Weygart 1996, Kudlicki et al. 2000). In numerical analyses, a mass-weighted smoothing is a straightforward and convenient approach. In the followings we perturbatively investigate this approach (Seto 2000b for details).

We consider particles' system mimicing N-body simulations. Particles are initially placed at grid points of the orthogonal (Lagrangian) coordinate system \mathbf{q} . We assume that each particle has equal mass $m(N)$ (N ; number of particles in a simulation box). The simplest numerical method for calculating a smoothed velocity field (say at a point \mathbf{x}_0) contains two steps. The first step is to sum up peculiar velocities of particles $\mathbf{V}(\mathbf{x}(\mathbf{q}_i))$ with weight $W(\mathbf{x}(\mathbf{q}_i) - \mathbf{x}_0; R)$ determined by their distances to the point \mathbf{x}_0 in interest. The sum represents “momentum density” rather than “velocity”. Thus the second step is to divide this sum with smoothed density at point \mathbf{x}_0 . We denote the final smoothed velocity field obtained in this manner by $\mathbf{V}_{mass}(\mathbf{x}_0, R)$. It is expressed as follows:

$$\mathbf{V}_{mass}(\mathbf{x}_0, R) = \frac{m(N) \sum_i^N \mathbf{V}(\mathbf{x}(\mathbf{q}_i)) W(\mathbf{x}(\mathbf{q}_i) - \mathbf{x}_0; R)}{m(N) \sum_i^N W(\mathbf{x}(\mathbf{q}_i) - \mathbf{x}_0; R)}. \quad (18)$$

If we increase the total number of particles N with keeping their mean density $\bar{\rho}$, we can replace the summation $m(N) \sum_i^N$ by three-dimensional integral with respect to the Lagrangian coordinate \mathbf{q} . Next we change the coordinate system from Lagrangian \mathbf{q} to Eulerian \mathbf{x} and obtain the following result as

$$\lim_{N \rightarrow \infty} m(N) \sum_i^N \mathbf{V}(\mathbf{x}(\mathbf{q}_i)) W(\mathbf{x}(\mathbf{q}_i) - \mathbf{x}_0, R) = \int d^3 q \bar{\rho} W(\mathbf{x}(\mathbf{q}) - \mathbf{x}_0; R) \mathbf{V}(\mathbf{x}(\mathbf{q})) \quad (19)$$

$$= \int d^3 x W(\mathbf{x} - \mathbf{x}_0; R) \bar{\rho} \{1 + \delta(\mathbf{x})\} \mathbf{V}(\mathbf{x}) \quad (20)$$

$$= \bar{\rho} \{[\mathbf{V}(\mathbf{x}_0)]_R + [\mathbf{V}(\mathbf{x}_0) \delta(\mathbf{x}_0)]_R\}, \quad (21)$$

where we have used the well-known fact that Jacobian $|\partial \mathbf{q} / \partial \mathbf{x}|$ of the coordinate transformation $\mathbf{q} \rightarrow \mathbf{x}$ is given by the local density $1 + \delta(\mathbf{x})$. As shown in the factor $1 + \delta(\mathbf{x})$ in equation (20), this

sampling is mass-weighted. In the same manner the denominator of equation (18) is given by

$$\lim_{N \rightarrow \infty} m(N) \sum_i^N W(\mathbf{x}(\mathbf{q}_i) - \mathbf{x}_0, R) = \bar{\rho}(1 + [\delta(\mathbf{x}_0)]_R). \quad (22)$$

In this case we can obtain the volume weighted quantity. With equations (20) and (22) the smoothed velocity field is expanded perturbatively as

$$\mathbf{V}_{mass}(\mathbf{x}, R) = [\mathbf{V}_1(\mathbf{x})]_R + [\mathbf{V}_2(\mathbf{x})]_R + [\mathbf{V}_1(\mathbf{x})\delta_1(\mathbf{x})]_R - [\mathbf{V}_1(\mathbf{x})]_R[\delta_1(\mathbf{x})]_R + O(\sigma^3). \quad (23)$$

The linear term $[\mathbf{V}_1(\mathbf{x})]_R$ is unaffected by the smoothing method. The second term represents the volume-weighted smoothed velocity field at the second-order of perturbations. Let us extract out the new second-order correction terms $\mathbf{V}_{2m}(\mathbf{x}, R)$ caused by the mass weighted smoothing as

$$\mathbf{V}_{2m}(\mathbf{x}, R) \equiv [\mathbf{V}_1(\mathbf{x})\delta_1(\mathbf{x})]_R - [\mathbf{V}_1(\mathbf{x})]_R[\delta_1(\mathbf{x})]_R. \quad (24)$$

Thus the velocity-density moment $\langle \mathbf{V} \cdot \mathbf{V} \delta \rangle$ for smoothed fields \mathbf{V}_{mass} and δ_R is written as

$$\langle \mathbf{V}_{mass}^2 \delta_R \rangle = \langle \mathbf{V}_R^2 \delta_R \rangle + 2 \langle \mathbf{V}_{1R} \cdot \mathbf{V}_{2m} \delta_{1R} \rangle. \quad (25)$$

The first term is given in the previous subsection up to the required order of σ (see eq.[13]). The additional term caused by the mass-weighted smoothing is evaluated in terms of the power spectrum as

$$\begin{aligned} 2 \langle [\mathbf{V}]_R \cdot \mathbf{V}_{2m} \delta_R \rangle &= 2H^2 f^2 \int \frac{d^3 k d^3 l}{(2\pi)^6} P(k) P(l) \left\{ \frac{1}{k^2} + \frac{\mathbf{k} \cdot \mathbf{l}}{k^2 l^2} \right\} \\ &\quad \times \{ \exp(-(k^2 + l^2 + \mathbf{k} \cdot \mathbf{l})) - \exp(-(k^2 + l^2)) \}. \end{aligned} \quad (26)$$

For power-law models ($P(k) \propto k^n$) the correction term ΔC_M caused by the above expression for the factor C is written with Hypergeometric functions (Seto 2000b)

$$\begin{aligned} \Delta C_M = \frac{2 \langle [\mathbf{V}]_R \cdot \mathbf{V}_{2m} \delta_R \rangle}{\langle \mathbf{V}_R^2 \rangle \langle \delta_R^2 \rangle} &= 2F\left(\frac{n+1}{2}, \frac{n+3}{2}, \frac{3}{2}, \frac{1}{4}\right) - \frac{(1+n)}{3}F\left(\frac{n+3}{2}, \frac{n+3}{2}, \frac{5}{2}, \frac{1}{4}\right) \\ &\quad - 2F\left(\frac{n+1}{2}, \frac{n+3}{2}, \frac{3}{2}, 0\right). \end{aligned} \quad (27)$$

The values of this correction term for various n 's are shown in table 1.

2.3. Adaptive Smoothing

It has been pointed out that cosmic fields might be resolved more efficiently by using adaptive smoothing filters than traditional spatially fixed filters (*e.g.* Springel et al. 1998). Seto (2000b,c) studied second-order effects of this method for various moments of density and velocity fields. In the adaptive method the smoothing radius is determined by local density. We use a larger smoothing

radius at the sparse underdense region but use a smaller one at the high density region where nonlinear effects would be larger. Therefore, the perturbative treatment for the adaptive method might break down faster and its performance should be checked numerically. In this subsection we summarize second-order effects caused by the adaptive smoothing (Seto 2000b,c). Our analytical results are compared with numerical ones in §4.

We first determine the adaptive smoothing radius so that number of particles within the radius becomes constant. This condition is written as

$$R(\mathbf{x})^3[1 + \delta(\mathbf{x})]_{R(\mathbf{x})} = R^3 = \text{const}, \quad (28)$$

where R is the standard smoothing scale. We can perturbatively solve this equation for the adaptive radius $R(\mathbf{x})$ and obtain ¹

$$R(\mathbf{x}) = R \left(1 - \frac{[\delta(\mathbf{x})]_R}{3} + O(\sigma^2) \right). \quad (29)$$

There are mainly two approaches for the adaptive smoothing, namely, the gather approach and the scatter approach (Hernquist & Katz 1989). Here we adopt the gather approach and basically calculate smoothed fields using operator $[\cdot]_{R(\mathbf{x})}$. After some algebra we obtain the second-order correction for the smoothed density field caused by the adaptive filter

$$\delta_{2A}(\mathbf{x}, R) = -\frac{R}{3} \delta_{1R}(\mathbf{x}) \frac{\partial}{\partial R} \delta_{1R}(\mathbf{x}) + \frac{R}{6} \frac{d}{dR} \langle \delta_{1R}^2 \rangle, \quad (30)$$

where the second term of the right-hand-side comes from the requirement $\langle \delta_{2A} \rangle = 0$. This correction term gives new contribution ΔS_{3A} to the skewness parameter S_3 as

$$\Delta S_{3A} = \frac{3 \langle \delta_{2A}(\mathbf{x}, R) \delta_{1R}(\mathbf{x})^2 \rangle}{\langle \delta_{1R}^2 \rangle^2} \quad (31)$$

$$= -\frac{\langle \delta_{1R}^2 \rangle R \partial_R \langle \delta_{1R}^2 \rangle}{\langle \delta_{1R}^2 \rangle^2} \quad (32)$$

$$= n + 3, \quad (33)$$

where we have used relation $\langle \delta_{1R}^2 \rangle \propto R^{-(n+3)}$ for power-law models. As we can see from above derivation, the term ΔS_{3A} does not depend on the filter functions.

In the same manner the additional second-order terms for the smoothed velocity field is given as

$$\mathbf{V}_{2A}(\mathbf{x}, R) = -\frac{R^2}{3} \delta_{1R}(\mathbf{x}) \nabla^2 \mathbf{V}_{1R}(\mathbf{x}). \quad (34)$$

We evaluate the new contribution ΔC_A for the coefficient C caused by this correction term² and obtain following result for power-law models as

$$\Delta C_A = -\frac{2}{3} R^2 \frac{\langle \delta_{1R}^2 \rangle \langle \nabla^2 \mathbf{V}_{1R} \cdot \mathbf{V}_{1R} \rangle}{\langle \delta_{1R}^2 \rangle \langle \mathbf{V}_{1R}^2 \rangle} \quad (35)$$

¹In numerical analysis we use $R(\mathbf{x}) = R(1 + [\delta(\mathbf{x})]_R)^{-1/3}$.

²Note that the contribution $\langle \delta_{2A} \mathbf{V}_1^2 \rangle$ vanishes.

$$= -\frac{1}{3} \frac{\partial \ln \langle \mathbf{V}_{1R}^2 \rangle}{\partial \ln R} \quad (36)$$

$$= \frac{n+1}{3}, \quad (37)$$

where we have used relation valid for the Gaussian filter

$$\nabla^2 \mathbf{V}_{1R}(\mathbf{x}) = -\frac{1}{R} \frac{\partial \mathbf{V}_{1R}(\mathbf{x})}{\partial R}, \quad (38)$$

and a simple relation $\langle \mathbf{V}_{1R}^2 \rangle \propto R^{-(n+1)}$.

Since two second-order correction terms \mathbf{V}_{2m} and \mathbf{V}_{2A} are not coupled, their effects on moments C are simply additive. For example, if we perform the mass-weighted smoothing using the adaptive filter, the moment C becomes

$$C = C_V + \Delta C_M + \Delta C_A. \quad (39)$$

Same kind of additive relation holds for the skewness parameter.

3. SAMPLE VARIANCE

In the next section we numerically evaluate the factors C or S_3 using N-body simulations. For each run of simulations we calculate the volume average $A(Y, \mathcal{V})$ of a field $Y(\mathbf{x})$ within the simulation box (cube) \mathcal{V} as follows:

$$A(Y, \mathcal{V}) \equiv \frac{1}{\mathcal{V}} \int Y(\mathbf{x}) d^3x. \quad (40)$$

The ensemble average $\langle A(Y, \mathcal{V}) \rangle$ of the estimator $A(Y, \mathcal{V})$ coincides with the ensemble average $\langle Y(\mathbf{x}) \rangle$ of the original field $Y(\mathbf{x})$ and we have

$$\langle A(Y, \mathcal{V}) \rangle = \langle Y(\mathbf{x}) \rangle. \quad (41)$$

But the measured value $A(Y, \mathcal{V})$ fluctuates around its mean value $\langle Y(\mathbf{x}) \rangle$ due to finiteness of the simulation box. This fluctuation can become important for analysis of numerical simulations. We call the root-mean-square value $D(Y, \mathcal{V})$ of this fluctuation as the sample variance

$$D(Y, \mathcal{V})^2 \equiv \langle (A(Y, \mathcal{V}) - \langle Y \rangle)^2 \rangle. \quad (42)$$

In this subsection we discuss the sample variances of various moments following Seto & Yokoyama (2000). The sample variance is closely related to the number of statistically independent regions that is roughly determined by the correlation length of the field $Y(\mathbf{x})$ and the size of the simulation box (or survey volume). Effects of the sample variance is generally more important for the velocity field than the density field, as the former is more weighted to large-scale fluctuations and has a larger correlation length.

For fields $Y(\mathbf{x}) = \mathbf{V}(\mathbf{x})^2\delta(\mathbf{x})$ and $Y(\mathbf{x}) = \delta(\mathbf{x})^3$ we have vanishing means $\langle \delta(\mathbf{x})\mathbf{V}(\mathbf{x})^2 \rangle = 0$ and $\langle \delta(\mathbf{x})^3 \rangle = 0$ at the linear order of perturbations as explained before³. However their sample variances do not vanish at the linear order and we have the following relation for relative fluctuations of their measured value $A(Y, \mathcal{V})$

$$\frac{D(Y, \mathcal{V})}{\langle Y \rangle} = O(\sigma^{-1}). \quad (43)$$

In contrast both the expectation values and the sample variances for the second moments $Y(\mathbf{x}) = \delta(\mathbf{x})^2$ or $Y(\mathbf{x}) = \mathbf{V}(\mathbf{x})^2$ have contributions from the linear modes and we have

$$\frac{D(Y, \mathcal{V})}{\langle Y \rangle} = O(1). \quad (44)$$

In the weakly nonlinear regime, the sample variance of the factor $C \equiv \langle \mathbf{V}^2\delta \rangle / (\langle \mathbf{V}^2 \rangle \langle \delta^2 \rangle)$ would be dominated by fluctuations of the numerators $\langle \mathbf{V}^2\delta \rangle$, as expected from equations (43) and (44).

Here we evaluate the sample variance $D(Y, \mathcal{V})$ caused by the linear modes for the moment $Y(\mathbf{x}) = \mathbf{V}(\mathbf{x})^2\delta(\mathbf{x})$. We assume that our simulation box is a cube with side length L . After some algebra the sample variance can be written as

$$\begin{aligned} D(\mathbf{V}^2\delta, \mathcal{V})^2 &= \frac{2H^4}{L^9} \sum_{\mathbf{k}} \sum_{\mathbf{l}} P(k)P(l)P(|\mathbf{k} + \mathbf{l}|)W(kR)^2W(lR)^2W(|\mathbf{k} + \mathbf{l}|)^2 \\ &\times \frac{\mathbf{k} \cdot \mathbf{l}}{k^2l^2} \left\{ \frac{\mathbf{k} \cdot \mathbf{l}}{k^2l^2} - 2\frac{\mathbf{k} \cdot (\mathbf{k} + \mathbf{l})}{k^2(\mathbf{k} + \mathbf{l})^2} \right\}, \end{aligned} \quad (45)$$

where the wave vector \mathbf{k} is expressed as $\mathbf{k} = 2\pi/L(n_x, n_y, n_z)$ with integers n_x, n_y and n_z . Now let us approximate the above expression by replacing the summations with integrals, because it is not easy to evaluate these summations. We introduce the large-scale cut-off at wave-number $k_{min} = 2\pi/L$ that is determined by the side length L of the simulation box \mathcal{V} . Then we obtain

$$\begin{aligned} D(\mathbf{V}^2\delta, \mathcal{V})^2 &\simeq \frac{2H^4}{(2\pi)^6 L^3} \int_{k_{min}} d^3k \int_{k_{min}} d^3l P(k)P(l)P(|\mathbf{k} + \mathbf{l}|)W(kR)^2W(lR)^2W(|\mathbf{k} + \mathbf{l}|)^2 \\ &\times \frac{\mathbf{k} \cdot \mathbf{l}}{k^2l^2} \left\{ \frac{\mathbf{k} \cdot \mathbf{l}}{k^2l^2} - 2\frac{\mathbf{k} \cdot (\mathbf{k} + \mathbf{l})}{k^2(\mathbf{k} + \mathbf{l})^2} \right\}. \end{aligned} \quad (46)$$

Due to the rotational symmetry around the origin this integral is simplified to a three-dimensional integral. In the same manner the sample variance for the third-order moments of density field is given as follows:

$$D(\delta^3, \mathcal{V})^2 \simeq \frac{6}{(2\pi)^6 L^3} \int_{k_{min}} d^3k \int_{k_{min}} d^3l P(k)P(l)P(|\mathbf{k} + \mathbf{l}|)W(kR)^2W(lR)^2W(|\mathbf{k} + \mathbf{l}|)^2. \quad (47)$$

³In this section we drop the subscript R (smoothing radius) and simply denote $\mathbf{V}(\mathbf{x}) = [\mathbf{V}(\mathbf{x})]_R$ and $\delta(\mathbf{x}) = [\delta(\mathbf{x})]_R$.

For the second moments $\langle \mathbf{V}(\mathbf{x})^2 \rangle$ or $\langle \delta(\mathbf{x})^2 \rangle$ we have the following results

$$D(\mathbf{V}^2, \mathcal{V})^2 \simeq \frac{2H^4}{(2\pi)^3 L^3} \int_{k_{min}} d^3 k P(k)^2 W(kR)^4 k^{-4}, \quad D(\delta^2, \mathcal{V})^2 \simeq \frac{2}{(2\pi)^3 L^3} \int_{k_{min}} d^3 k P(k)^2 W(kR)^4. \quad (48)$$

In this section we made a crude estimation of the sample variance $D(Y, \mathcal{V})$. We have only studied the fluctuations caused by the linear modes and used approximation of replacing summations with integrals. Therefore our estimation is not quantitatively correct. However the present analysis would be useful to interpret numerical results given in the next section.

4. NUMERICAL ANALYSIS

We performed P³M N-body simulations using 64^3 particles in a cube with side length $L = 1$. The numerical code is provided by Couchman. We firstly investigated two scale-free models with spectral indexes $n = 1$ and 0 in Einstein de-Sitter background and run several simulations for each models. We stopped calculations at the epoch when the matter fluctuation at the smoothing radius $R = 1/80$ (R : the smoothing radius for the Gaussian filter) becomes $\sigma_R^2 \simeq 2$ for the $n = 0$ model and $\sigma_R^2 \simeq 1$ for the $n = 1$ model. Before describing numerical results, we mention two important effects that must be cared here. The first one is the sample variance described in the previous section and the second one is the artificial cut-offs induced in the initial fluctuations.

We are interested in the velocity and density fields at weakly nonlinear regimes. As explained before, the sample variances of various statistical quantities become larger for a larger smoothing radius. In figure 1 we estimated the relative fluctuations $D(Y, \mathcal{V})/\langle Y \rangle$ caused by the linear modes using expressions given in §3 at the final epoch of each simulation. Apparently, the moment $\langle \mathbf{V}^2 \delta \rangle$ has the largest fluctuations. The fluctuation can be as much as the expectation value itself, i.e., 100% variance for smaller $\sigma^2(R)$. The sample variance is very sensitive to the large-scale fluctuations. Roughly speaking, the sample variance is more important for $n = 0$ model than for $n = 1$ model, as the former has more large-scale powers. Because of the same reason, the velocity dispersion $\langle \mathbf{V}^2 \rangle$ has larger fluctuations than the variance of density fluctuations $\langle \delta^2 \rangle$.

There are two cut-off scales for initial matter fluctuations in our simulations. One is the Nyquist frequency $k_{Nyq} = \pi N/L$ determined by the initial separation of particles and the other one is the wave number k_{min} determined by the side length of the simulation box as $k_{min} = 2\pi/L$. Our analytical predictions given in §2 might be different from numerical results due to these artificial cut-offs. To estimate their effects we calculate the factors C_V and ΔC_M with a modified power spectra $P_{eff}(k)$ mimicing N-body simulations as follows (e.g. Seto 1999):

$$P_{eff}(k) = \begin{cases} 0 & (0 \leq k < k_{min}) \\ k^n & (k_{min} \leq k \leq k_{Nyq}) \\ 0 & (k_{Nyq} < k). \end{cases} \quad (49)$$

Analysis for the $n = -1$ model is particularly interesting as we have $C_V = \Delta C_M = \Delta C_A = 0$ and velocity dispersion does not depend on the density contrast even at the second-order of perturbation. However, the wave-number integral (eq.[10]) for the velocity dispersion diverges in the $k \rightarrow 0$ limit and the velocity field would be strongly affected by the artificial large-scale cut-off at k_{min} . Actually we have confirmed numerically that the factors C_V and ΔC_M for this model with the modified spectrum $P_{eff}(k)$ would considerably deviate from the original scale-free model. We apply this analysis for models with indexes $n = 0$ and 1 , and found that the factors C_V and ΔC_M could deviate largely from predictions for the original scale-free models at $R \lesssim 1/80$ or $R \gtrsim 1/20$. Thus we limit our analysis only for smoothing radius with $1/80 \leq R \leq 1/20$.

We have analyzed N-body data at the final epoch for each run. As our simulations are basically self similar, we can expect that physics is characterized only by the magnitude of nonlinearity $\sigma^2(R) = \langle \delta_R^2 \rangle$. Thus we use the variance $\sigma^2(R)$ rather than the radius R to represent the scale dependence. For $n = 0$ model we have performed three runs. Our numerical results are given in figure 2. In the upper left panel the factors S_{3V} and C are shown as a function of nonlinearity $\sigma^2(R)$. The symbols represent the average values of three runs and the error bars are the variances of their fluctuations. The magnitude of error bars is roughly understood by checking the sample variances caused by the linear modes given in figure 1 where we have added numerical results from simulations for the quantity $\langle \mathbf{V}^2 \delta \rangle$.

As shown in literatures (*e.g.* Hivon et al. 1995, Juszkiewicz et al. 1995, Lokas et al. 1995), the skewness parameter S_{3V} at $\sigma^2(R) \lesssim 1$ is nearly constant for $n = 1$ model and close to the predictions of the second-order perturbation theory $S_{3V} = 3.14$. In contrast the factor C depends strongly on nonlinearity $\sigma^2(R)$ and we have $C \simeq 0.05$ at $\sigma^2(R) \simeq 1$. This value is only $\simeq 40\%$ of the second-order prediction $C = 0.12$. The numerical results for C become close to the analytical prediction at $\sigma^2(R) = 0.2$ where the sample variance is fairly large. In figure 2 we also show the constrained velocity dispersion $\Sigma_V^2(\delta)/\sigma_V^2$ in the range of density contrast $-1.5\sigma(R) \leq \delta \leq 1.5\sigma(R)$. We have made a same kind of averaging operation for three runs as in the case of the factors S_{3V} and C . The dashed lines are the analytical predictions given in equation (7) whose slope is $C \simeq 0.12$. The numerical results is close to the analytical prediction at small $\sigma^2(R)$, but the slope of numerical results become smaller for larger $\sigma(R)$ as expected form behavior of the factor C .

Let us show same analyses for the model with $n = 1$. For this model we performed seven runs. Results are shown in figure 3. The measured parameter S_{3V} is nearly constant but somewhat ($\simeq 10\%$) smaller than the analytical prediction $S_{3V} = 3.03$. The factor C is again a decreasing function of nonlinearity $\sigma^2(R)$. However its convergence to the analytical prediction $C = 0.2$ seems to be slower. Even at $\sigma^2(R) = 0.04$ where the sample variance is considerably large, the measured value is much smaller than the analytical one. The constrained velocity dispersion $\Sigma_V^2(\delta)$ behaves in the same manner as the model with $n = 0$. The effective slope becomes smaller for larger $\sigma^2(R)$. The difference between the second-order prediction and the numerical results is caused by the nonlinear effects that cannot be traced by the second-order perturbation. For given $\sigma^2(R)$ this difference is larger for the model with $n = 1$ than the one with $n = 0$. This is reasonable as

the former has more small scale power initially and nonlinear effects would be larger. Nagamine, Ostriker & Cen (2000) have numerically studied the cosmic Mach number (Ostriker & Suto 1990) as a function of overdensity using an LCDM hydrodynamical simulation. They have provided two-dimensional contour plots for the probability distribution functions of the smoothed dark-matter overdensity δ_R and the bulk velocity $|\mathbf{V}_R|$ at various smoothing scales $R = 5, 10$ and $20h^{-1}\text{Mpc}$ (see their figures 10-12). Comparing these figures we can observe the scale dependence of $\Sigma_V^2(\delta)$ discussed so far.

We have also performed N-body simulations (5 runs) for a CDM model. Our model parameters are fixed at $\Omega_0 = 1.0$, $h = 0.5$ ⁴ and the CDM shape parameter $\Gamma = 0.5$. We used the CDM transfer function of Bardeen et al. (1986) with the primordially $n = 1$ spectrum and normalized the linear spectrum by $\sigma_8 = 0.8$ (σ_8 is the rms density fluctuation within a top-hat sphere of radius $8h^{-1}\text{Mpc}$). As the velocity field is heavily weighted to large-scale fluctuations, we have adopted a $L = 400h^{-1}\text{Mpc}$ simulation box. The prediction C by the second-order theory at the weakly nonlinear regime is $C \sim 0.13$ and close to the previous result for the $n = 0$ model. Our numerical results are $C = 0.094 \pm 0.06$ for $R = 10h^{-1}\text{Mpc}$ ($\sigma^2(R) = 0.07$), and $C = 0.068 \pm 0.01$ for $R = 5h^{-1}\text{Mpc}$ ($\sigma^2(R) = 0.37$), which are consistent with the prediction of the second-order theory. The mean values and the error bars depend on nonlinearity σ_R^2 as in the case of the $n = 0$ model.

Hui & Gaztañaga (1999) have pointed out that a nonlinear combination f of estimators $A(Y_i, \mathcal{V})$ (see eq.[40]) should be analyzed with sufficient care. We have following inequality even in the case of the unbiased estimators $\langle A(Y_i, \mathcal{V}) \rangle = \langle Y_i \rangle$:

$$f(\langle Y_1 \rangle, \dots, \langle Y_n \rangle) = f(\langle A(Y_1, \mathcal{V}) \rangle, \dots, \langle A(Y_n, \mathcal{V}) \rangle) \neq \langle f(A(Y_1, \mathcal{V}), \dots, A(Y_n, \mathcal{V})) \rangle. \quad (50)$$

This inequality leads to a biased estimation for the nonlinear function $f(\langle Y_i \rangle)$. When the variance $\bar{\xi}_2^{\mathcal{V}}$ of density contrast smoothed in survey volume \mathcal{V} is much smaller than unity, this bias ΔS_{3V} for the estimation of the skewness S_{3V} is approximately given as follows (Hui & Gaztañaga 1999)

$$\frac{\Delta S_{3V}}{S_{3V}} = \alpha_1 \frac{\bar{\xi}_2^{\mathcal{V}}}{\langle \delta_R^2 \rangle} + \alpha_2 \bar{\xi}_2^{\mathcal{V}}, \quad (51)$$

where the coefficients $\{\alpha_i\}$ are determined by the power spectrum. As we use data in full simulation boxes, there are no mean density fluctuations $\bar{\xi}_2^{\mathcal{V}} = 0$ and the above expansion (51) vanishes. Therefore we evaluate the estimation bias by directly comparing numerical values $f(\langle A(Y_1, \mathcal{V}) \rangle, \dots, \langle A(Y_n, \mathcal{V}) \rangle)$ and $\langle f(A(Y_1, \mathcal{V}), \dots, A(Y_n, \mathcal{V})) \rangle$ (the ensemble average $\langle \cdot \rangle$ is taken for different realizations of simulations). We find that differences between these two are very small both for S_V and C_V . For data presented in figures 2 and 3 the difference is smaller than 1%. This is due to the fact that the fluctuations of their denominators (expressed by $\langle \delta^2 \rangle$ and $\langle \mathbf{V}^2 \rangle$) are very small as expected from figure 1. This estimation bias would be more important in actual observational situations.

⁴As commented in §2.1, our results for the parameter C would depends weakly on the background cosmological parameters.

In figure 4 we present numerical results for the factors S_3 and C that were evaluated using the adaptive filter described in §2.3. As shown in the left panels, the skewness parameter S_3 shows reasonable agreement with the second-order perturbation theory. But the parameter C again shows strong dependence on nonlinearity $\sigma^2(R)$ even in this regime and its convergence to the analytical prediction is slow. These behaviors of S and C are similar to the previous case of non-adaptive smoothing. The parameter C for the model with $n = 0$ becomes close to the second-order result $C = 0.45$. For $n = 1$ model, the second-order correction $\Delta C_A = 0.67$ caused by the adaptive smoothing seems not to match the numerical result even at the scale $\sigma^2 \simeq 0.04$. In the adaptive method we use a smaller smoothing radius at high density regions. Thus numerical results are expected to be more contaminated by strongly nonlinear effects than the previous simple smoothing method especially for $n = 1$ model. The numerical result is estimated as $\Delta C_A \simeq 0.44$ from $C_V + \Delta C_M + \Delta C_A = 0.56$ (figure 4) and $C_V + \Delta C_M = 0.12$ (figure 3).

Finally we comment on possibility of the determination of the parameter C_V by the actual observations. As only the line-of-sight velocity field $V_{||}(\mathbf{x})$ is observable, we evaluate the fluctuations of linear modes for the moment $\langle V_{||}^2 \delta \rangle$. For this evaluation we cannot simply apply results derived under the periodic boundary condition in §3. We estimate the sample variance $D(V_{||}^2 \delta, \mathcal{V})$ using a method similar to Seto & Yokoyama (2000). As an example we have examined a flat cold-dark-matter model with cosmological parameters $h = 0.7$, $\Omega_0 = 0.3$ and $\lambda_0 = 0.7$. Normalization of the power spectrum is determined by abundance of rich clusters as $\sigma_8 = 0.50 \Omega_0^{-0.53+0.13\Omega_0}$ (Eke, Cole & Frenk 1996). The Gaussian smoothing radius is fixed at $R = 12h^{-1}\text{Mpc}$. The second-order prediction of the parameter C for the primordially scale-invariant CDM power spectrum in a weakly nonlinear regime is close to that for the $n = 0$ model. Therefore we assume

$$\langle V_{||}^2 \delta \rangle = \frac{\langle \mathbf{V}^2 \delta \rangle}{3} \simeq \frac{C \langle \mathbf{V}^2 \rangle \langle \delta^2 \rangle}{3} \simeq 0.04 \langle \mathbf{V}^2 \rangle \langle \delta^2 \rangle. \quad (52)$$

Using these relations we obtain $D(V_{||}^2 \delta, \mathcal{V}) / \langle V_{||}^2 \delta \rangle \sim 8$ for a spherical volume with survey depth $80h^{-1}\text{Mpc}$. Thus we can hardly measure the parameter C from current catalogs of peculiar velocity field, such as, Mark III (Willick et al. 1997) or SFI (Haynes et al. 1998). The relative fluctuation becomes close to unity only at a survey volume with depth $\sim 300h^{-1}\text{Mpc}$. In the actual observational situations the effects caused by the nonlinear estimators (eq.[50]) would be also important.

5. SUMMARY

We have investigated various statistical quantities of smoothed velocity and density fields. Analytical predictions based on second-order perturbation theory are compared with numerical results obtained from N-body simulations. Our primary target is the velocity dispersion $\Sigma_V^2(\delta)$ as a function of local density contrast δ at weakly nonlinear scales. At the linear order with isotropic random Gaussian initial condition the dispersion $\Sigma_V^2(\delta)$ does not depend on δ . However second-

order modes generate a correction term proportional to δ with its slope $C \equiv \langle \mathbf{V}^2 \delta \rangle / (\langle \mathbf{V}^2 \rangle \langle \delta^2 \rangle)$. We have confirmed this dependence at small $\sigma(R)$ and found that the parameter C depends largely on nonlinearity $\sigma(R)$ even in the regime where the skewness parameter S_3 is nearly constant value and close to prediction by second-order perturbation theory.

We have also studied second-order effects caused by various smoothing methods. Proper treatment of smoothing is crucial to quantitatively discuss weakly nonlinear effects of cosmic fields. A mass weighted smoothing is convenient to analyze velocity field traced by particles as in N-body simulations. We have basically used this method for our numerical analysis. We found that the parameter C actually approaches to the value that includes effects of mass-weighted smoothing in the limit of small $\sigma(R)$. But a large smoothing radius is required to recover the second-order result. For example we have to take the radius R with $\sigma^2(R) \lesssim 0.1$ for the $n = 0$ model and $\sigma^2(R) \lesssim 0.01$ for the $n = 1$ model. Adaptive smoothing methods might be useful to resolve cosmic field especially in underdense regions. The skewness parameter S_3 obtained numerically with an adaptive method (gather approach) is closed to the corresponding second-order prediction up to $\sigma^2(R) \simeq 1$. The skewness parameter and its generalizations are closely related to weakly nonlinear evolution of genus or area statistics of isodensity contour (Matsubara 1994) for which the adaptive method would be effective (Springel et al. 1998). Our result is encouraging for application of second-order analysis for density field smoothed by the adaptive filter.

It has been known that the second-order predictions at $\sigma(R) \simeq 1$ are more accurate for the skewness of the real space density field than that of the velocity divergence field $\propto \nabla \cdot \mathbf{V}$ (Juszkiewicz et al. 1995) or the redshift space density field (Hivon et al. 1995). But we should notice that calculation of the coefficient $C \equiv \langle \mathbf{V}^2 \delta \rangle / (\langle \mathbf{V}^2 \rangle \langle \delta^2 \rangle)$ directly requires information of the peculiar velocity field as a vector field. We found that performance of the second-order prediction is generally worse for the factor C than for the skewness S_3 . This fact seems interesting. As the density field is more weighted to the small-scale fluctuations than the velocity field, we can naively expect that highly nonlinear effects would be stronger for the density field. Therefore our numerical investigation provides applications of the second-order perturbation theory with an important caveat.

We thank Naoki Yoshida for discussion about numerical schemes and an anonymous referee for valuable comments to improve this manuscript. This work is supported by Japanese Grant-in-Aid for Science Research Fund of the Ministry of Education, Science, Sports and Culture Grant Nos. 0001461 and 11640235.

TABLE 1
VELOCITY-DENSITY MOMENT C (GAUSSIAN FILTER)

spectral index n	-1	0	1	2
C_V	0	0.24	0.31	0.38
ΔC_M	0	-0.12	-0.11	0.053
ΔC_A	0	0.33	0.67	1.0
$C_V + \Delta C_M$	0	0.12	0.20	0.43
$C_V + \Delta C_M + \Delta C_A$	0	0.45	0.87	1.43

TABLE 2
SKEWNESS S_3 (GAUSSIAN FILTER)

spectral index n	-1	0	1	2
S_{3V}	3.5	3.1	3.0	3.1
ΔS_{3A}	2.0	3.0	4.0	5.0
$S_{3V} + \Delta S_{3A}$	5.5	6.1	7.01	8.1

REFERENCES

Bardeen, J. M., Bond, J. R., Kaiser, N. & Szalay, A. S. 1986, *ApJ*, 305, 15

Baugh, C. M., Gaztañaga, E. & Efstathiou, G. 1996, *MNRAS*, 274, 1049

Bernardeau, F. 1994, *A&A*, 291, 697

Bernardeau, F. & van de Weygaert, R. 1996, *MNRAS*, 279, 693

Bernardeau, F. & Kofman L. 1995, *ApJ*, 443, 479

Bouchet, F. et al. 1992, *ApJ*, 394, L5

Cen, R. & Ostriker, J. P. 1992, *ApJ*, 399, L113

Chodorowski, M. & Lokas, E. L. 1997, *MNRAS*, 287, 591

Couchman, H. M. P. 1991, *ApJ*, 368, L23

Dekel, A. 1994, *ARA&A*, 32, 371

Eke, V. R., Cole, S. and Frenk, C. S. 1996, *MNRAS*, 282, 263

Fry, J. N. 1984, *ApJ*, 279, 499

Fry, J. N. & Gaztañaga, E. 1993, *ApJ*, 413, 447

Goroff, M. H., Grinstein, B., Rey, S. -J., & Wise, M. B., 1986, *ApJ*, 311, 6

Haynes, M. et al. 1998, *AJ*, 117, 1668

Hernquist, L. and Katz, N. 1989, *ApJS*, 70, 419

Hivon, E., Bouchet, F. R., Colombi, S. & Juszkiewicz, R. 1995, *A&A*, 298, 643

Hui, L. & Gaztañaga, E. 1999, *ApJ*, 519, 622

Juszkiewicz, R. Bouchet, F. & Colombi, S. 1993, *ApJ*, 412, L9

Juszkiewicz, R. et al. 1995, *ApJ*, 442, 39

Kaufmann, G., et al. 1999, *MNRAS*, 303, 188

Kepner, J. V., Summers, F. J. & Strauss, M. A. 1997, *New Astron.*, 2, 165

Kim, R. S. & Strauss, M. A. 1998, *ApJ*, 493, 39

Kudlicki, A. et al. 2000, *MNRAS*, 313, 464

Lahav, O., Rees, M. J., Lilje, P. B. & Primack, J. R. 1991, *MNRAS*, 251, 128

Łokas, E. L., Juszkiewicz, R., Weinberg, D. H. & Bouchet, F. R. 1995, MNRAS, 274, 730

Matsubara, T. 1994, ApJ, 434, L43

Nagamine, K. Ostriker, J. P. & Cen, R. 2000, preprint (astro-ph/0010253)

Narayanan, V. K., Berlind, A., & Weinberg, D. H. 2000, ApJ, 537, 537

Ostriker, J. P. & Suto, Y. 1990, ApJ, 348, 378

Peebles, P. J. E. 1980, The Large Scale Structure of the Universe (Princeton University Press: Princeton)

Seto, N. 1999, ApJ, 523, 24

Seto, N. 2000a, ApJ, 537, 21

Seto, N. 2000b, ApJ, 537, 525

Seto, N. 2000c, ApJ, 538, 11

Seto, N. & Yokoyama, J. 2000, PASJ, 52, 749

Springel, V. et al. 1998, MNRAS, 298, 1169

Strauss, M. & Willick, J. A. 1995, Phys.Rep., 261, 271

Willick, J. A. et al. 1997, ApJS, 109, 333

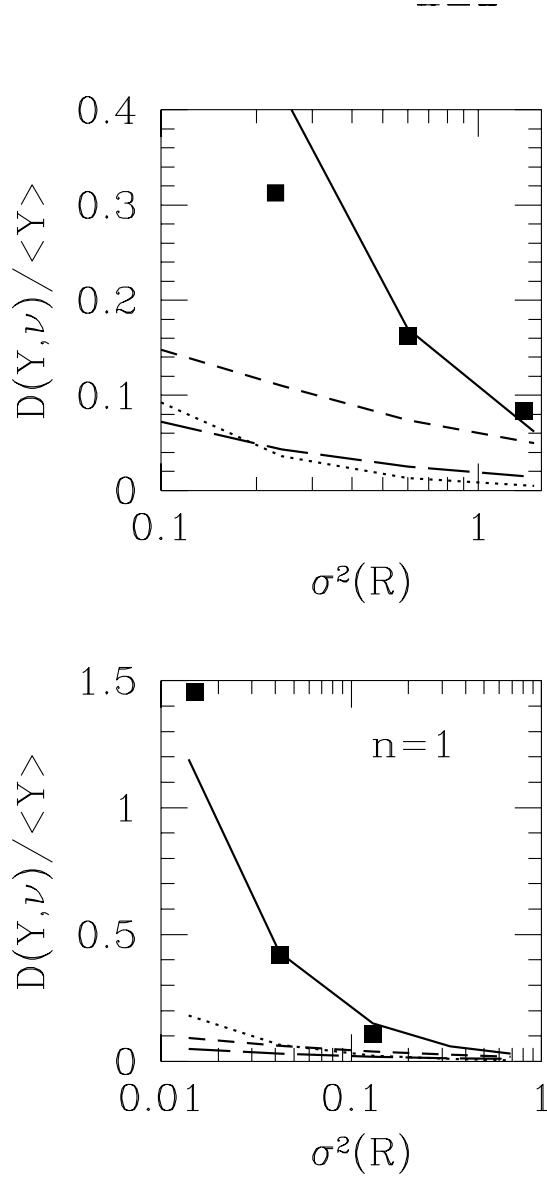


Fig. 1.— Relative fluctuations caused by the linear modes in our simulations (see §3 for their estimation). The solid lines correspond to the field $Y(\mathbf{x}) = \mathbf{V}(\mathbf{x})^2 \delta(\mathbf{x})$, the dotted to $Y(\mathbf{x}) = \delta(\mathbf{x})^3$, the short-dashed to $Y(\mathbf{x}) = \mathbf{V}(\mathbf{x})^2$ and the long-dashed to $Y(\mathbf{x}) = \delta(\mathbf{x})^2$. We numerically estimate the fluctuations $D(\mathbf{V}^2 \delta, \mathcal{V})$ from different realizations of simulation (see figures 2 and 3) and plot its relative magnitude with respect to the expectation value $\langle \mathbf{V}^2 \delta \rangle$ (predicted by the second-order perturbation theory) by the filled squares.

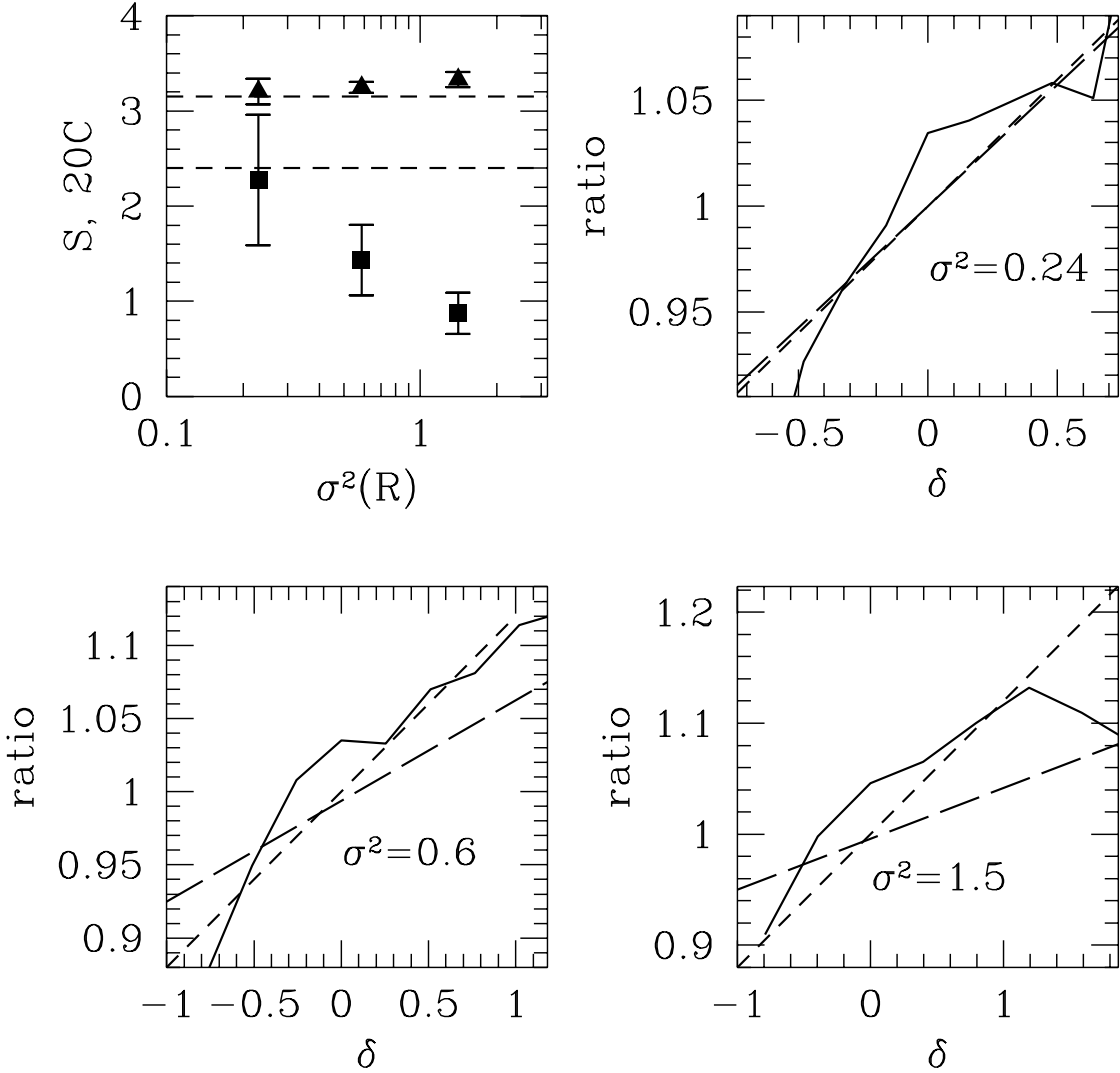


Fig. 2.— Two factors C , S_{3V} and the constrained bulk velocity dispersion $\Sigma_V^2(\delta)$ for $n = 0$ model. (1) Upper-left panel: The mean values (filled symbols) and error bars are obtained from three runs of simulations. The squares represent the factor C in the form of $20C$, and the triangles the skewness S_{3V} . Predictions by the second-order perturbation theory are shown by the dashed lines ($C = 0.12$ and $S_{3V} = 3.14$). (2) Other three panels: The constrained velocity dispersion is presented using the ratio $\Sigma_V^2(\delta)/\sigma_V^2$ in the range $-1.5\sigma(R) \leq \delta \leq 1.5\sigma(R)$. The short-dashed lines are predictions by the Edgeworth expansion method with the factor C from second-order perturbation theory, and the long-dashed lines are drawn with C obtained from numerical simulations.

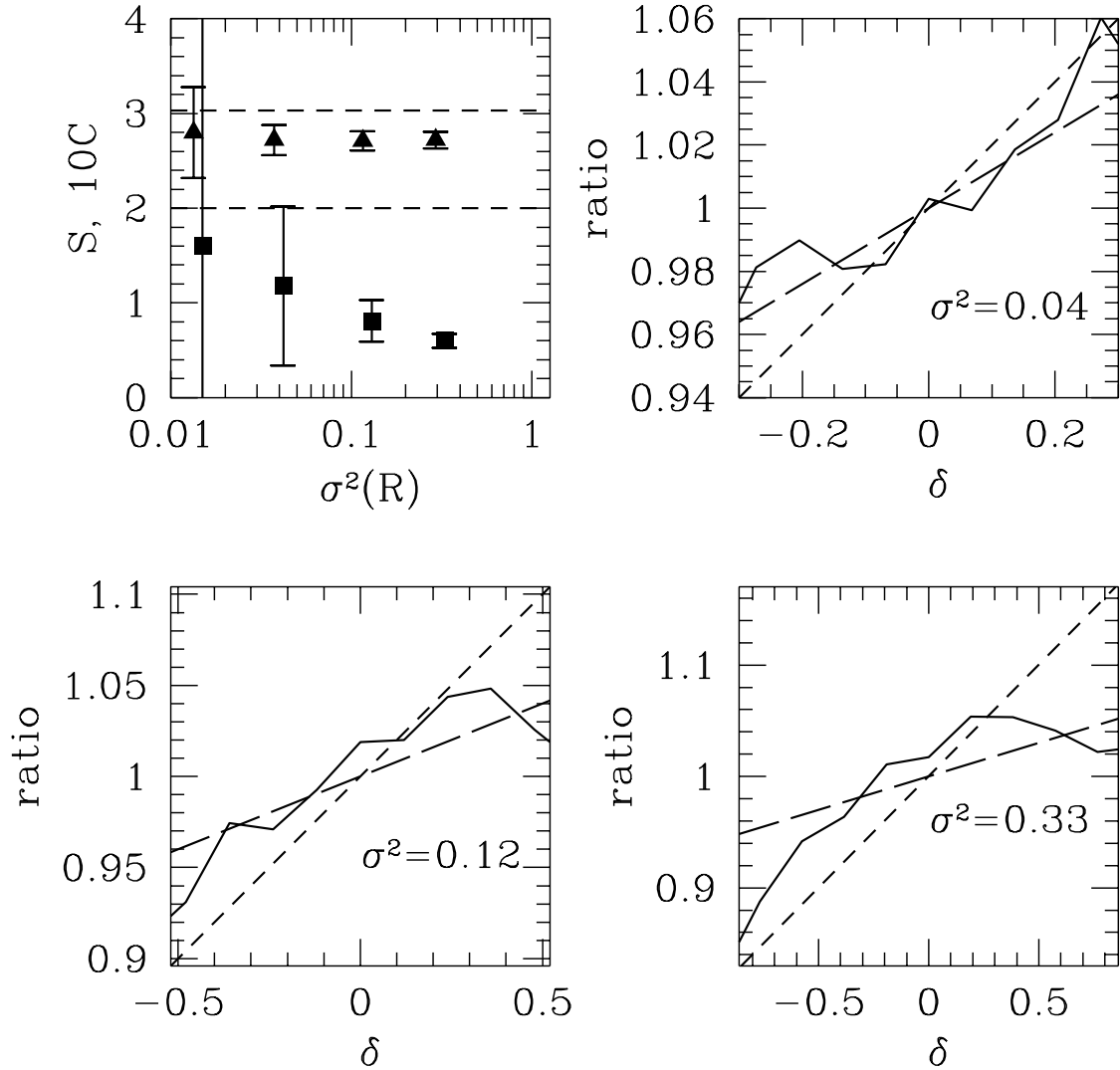


Fig. 3.— Numerical results for $n = 1$ model. Figures are given in the same manner as figure 2. Second-order perturbation predicts $C = 0.20$ and $S_{3V} = 3.03$.

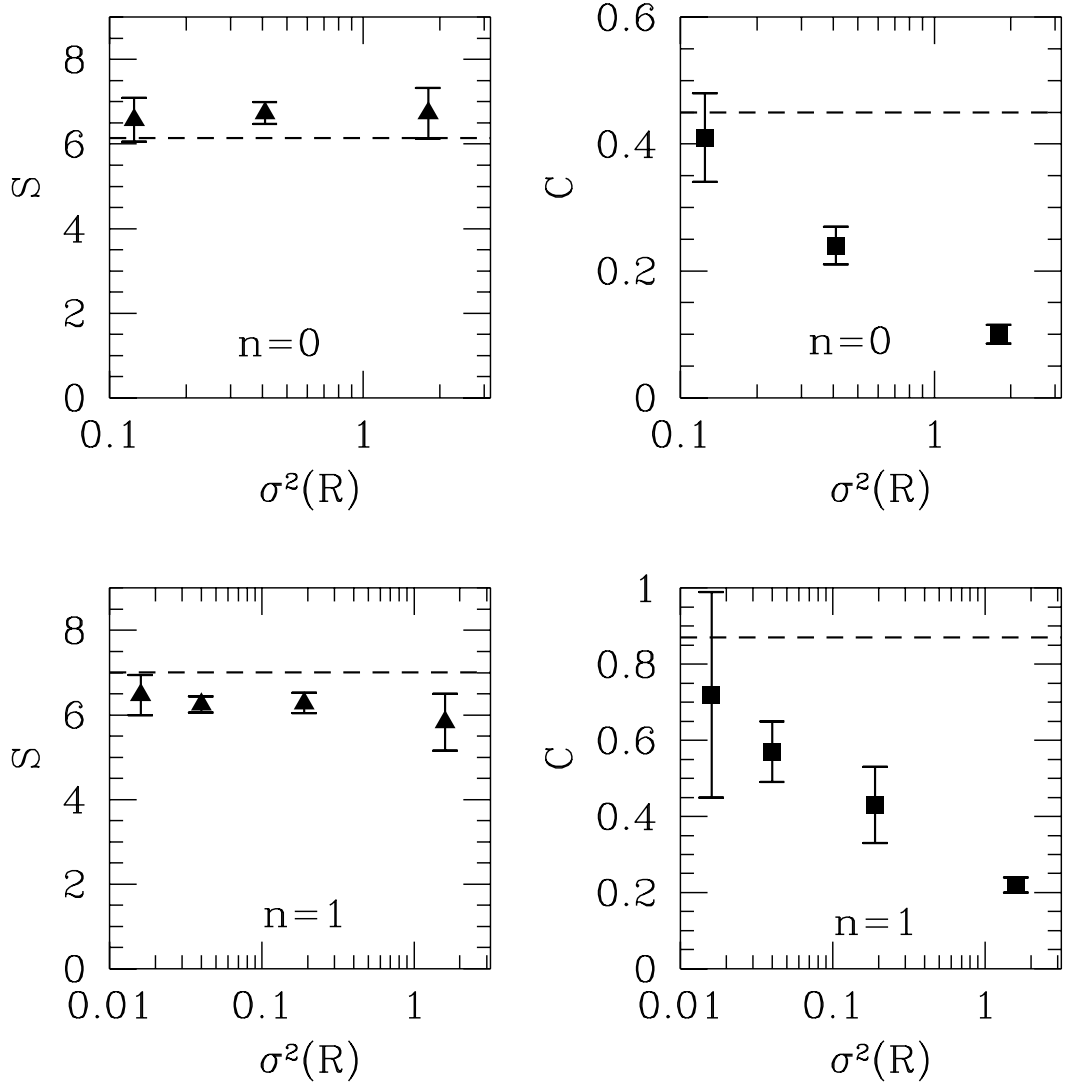


Fig. 4.— Effects of the adaptive smoothing for moments S_3 and C . We present the averaged values as in Figures 2 and 3. The upper panels correspond to $n = 0$ model and lower panels to $n = 1$ model. The dashed lines represent the second-order predictions: $S_3 = 6.1$, $C = 0.45$ for $n = 0$ model and $S_3 = 7.0$, $C = 0.87$ for $n = 1$ model.